Electron backscatter diffraction (EBSD) measurement of accumulated strain

Conference or Workshop Item

ELECTRON BACKSCATTER DIFFRACTION (EBSD) MEASUREMENT OF ACCUMULATED STRAIN

D. N. Githinji, S. M. Northover and P. J. Bouchard
Materials Engineering, The Open University, Walton Hall, Milton Keynes, MK7 6AA, UK

ABSTRACT
Reliable life prediction depends on a sound knowledge of the accumulated strain in components subject to creep. Electron backscatter diffraction (EBSD) is now well-established for estimating/measuring plastic strain and there have been a number of different EBSD metrics proposed for this. Microstructure has a strong effect on the calibration of most of these, limiting their use in critical areas such as around welds where microstructure is inhomogeneous. During the service life of materials such as 316 steel there is extensive precipitation but most published applications of EBSD are on precipitate-free materials. A systematic study has been made on the applicability of different EBSD metrics to both solution-annealed and service-aged 316H stainless steel subject to a range of plastic and creep strains between 0 and 35% to determine the conditions for maximum strain sensitivity of each. A simple new method of assessing cumulative strain, 'deformed grain fraction' (DGF) is presented and DGF has been compared with more conventional EBSD strain metrics. In 316H steel with a range of microstructures the effects of plastic and creep strains are additive for all metrics. DGF is relatively insensitive to changes in microstructure and its use is demonstrated in measuring total plastic strain in ex-service welded components.

INTRODUCTION
In many plants operating at high temperatures, such as those used in power generation, the safe operating life is limited by the creep of a few critical components and reliable methods of life prediction depend on a sound knowledge of both the operative mechanisms of deformation and damage and the plastic strain already accumulated. Welds present a particular problem because of their inhomogeneity in both microstructure and chemistry, combined with their localized residual plastic strain after cooling.

Several different metrics based on the sample-based surface technique of electron backscatter diffraction (EBSD)[1-6] have been developed to assess strain in materials such as 316 steel, widely used in power plants, when the material is in a solution-annealed condition, but no previous studies have been carried out to try and apply these metrics to aged materials containing significant precipitation. There has also been little previous comparison of the sensitivity of the different metrics in assessing strain over different ranges of strains. This study set out to address these questions and apply the results to ex-service welded 316H steel components.

EXPERIMENTAL
The major material used in this study was part of an ex-service power plant steam header that had been in service about 100,000h at around 789K (516^{o}C). It was AISI Type 316H stainless steel of average grain size 98±10μm. The full composition has been given elsewhere [6]. There was copious precipitation both at grain boundaries and within the grains.

Mechanical testing
Room temperature tensile (RTT), high temperature tensile (HTT), room temperature compression (RTC) and high temperature compression (HTC) tests were conducted on the as-received (ex-

service) material and room temperature tensile tests (SARTT) were also performed on material solution-treated for 1h at 1323K (1050°C) as detailed in Table 1.

Table 1: Mechanically tested specimen conditions

Test	% true plastic strain (ε)	Strain rate (s^{-1})	Temperature (°C)
RTT	5.1, 9.6, 14.1, 18.4, 22.5	$2.4x10^{-4}$	24
HTT	1.1, 3.1, 5.8, 9.5, 14, 17.4, 22.3	$3.5x10^{-5}$	550±1
RTC	6.32, 10.3, 14.1, 18.7,22.1	$5.0x10^{-4}$	24
HTC	5.8, 8.9, 14.3, 17.3, 23.6	$4.0x10^{-4}$	550±1
SARTT	3.1, 5.1, 9.7, 18.7	$3.5x10^{-3}$	550±1

Uniaxial creep tests under a constant load of 320MPa were also performed at 823K (550°C) up to a creep strain of 35%, using ex-service samples pre-strained at 823K by 8% (HTDC).

Weldment

A new weldment, consisting of pieces from two service-aged 316H steel headers, with a similar thermal history to that used in the main study, joined by manual metal arc welding using a 316L steel filler, was used to test the applicability of EBSD strain assessment techniques to the heat affected zones of welded components. Two 3mm thick slices of material in perpendicular directions (through the wall thickness and parallel to it) across the joint were extracted by electro-discharge machining (EDM). The geometry of the weld is shown in Fig.1. A cross-weld test specimen cut from the mid-section of the weld was also subjected to load-controlled creep testing at 818K with an applied stress of 315MPa. During the test the deformation was monitored using a high temperature digital image correlation technique[7] and the creep ruptured specimen was prepared for EBSD as described above.

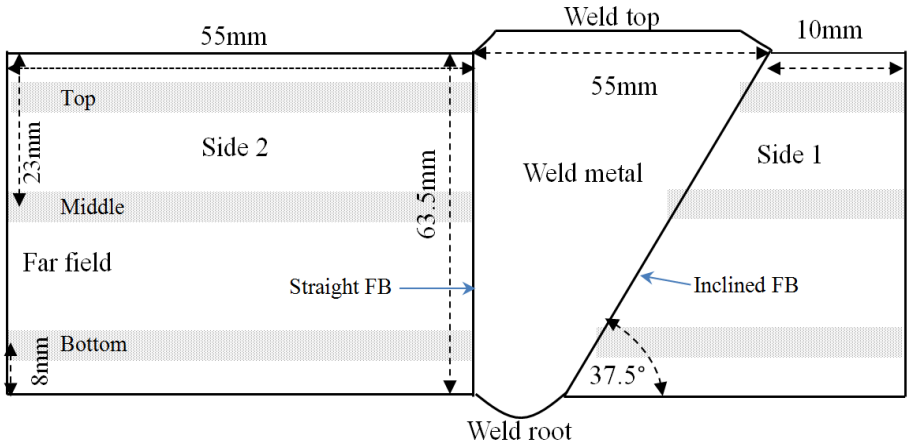

Fig.1Geometry of multi-pass weld of Type 316 stainless steel (EBSD measurement zones shaded)

EBSD measurements

Samples from undeformed ex-service steel, from each mechanically tested specimen and from the weld were examined using EBSD. Samples were cut by EDM and prepared by conventional mechanical polishing, followed by electro-polishing to remove all preparation-induced deformation. Details of this and of the data acquisition and post processing parameters optimized for maximum strain sensitivity are available elsewhere[6]. Deformation was seen to be very inhomogeneous so EBSD maps were acquired over 700μmx700μm areas. All maps used showed over 100 grains and had an indexing rate above 97%. In the case of the through-thickness welded

sample, the results from three adjacent orientation maps were combined for each measurement position. The conventional EBSD metrics used that consider very local misorientations within each grain were kernel average misorientation (KAM_a – the subscript indicating that the value is averaged over the whole mapped area) and what is usually called 'low angle boundary' fraction (LAB) but which should be more correctly be termed 'low angle misorientation' fraction (LAMF)[6]. The AMIS metric (Average MISorientation) evaluates the mean of all spatially uncorrelated misorientations in each grain, so looks at deformation on the grain scale rather than locally over 1-2μm as KAM_a and LAMF do. The accuracy of misorientation determination in conventional EBSD is about 0.5^o and this gives rise to misorientation 'noise' so that even in an undeformed grain the measured AMIS is non-zero. Because of their differing orientations relative to the operating stresses, in mechanical tests some grains will usually start to deform before others. Setting a threshold of the $AMIS_a$ measured in undeformed material it is possible to distinguish in an EBSD map between 'deformed' and 'undeformed' grains. The authors have recently proposed a new metric, Deformed Grain Fraction (DGF) [6], based on this and DGF has been found to be much less sensitive to variations in microstructure than KAM_a LAMF or $AMIS_a$.

RESULTS

Mechanically tested material

The flow curves from the tensile and creep tests of the different materials are shown in Fig.2. Figs 3 and 4 show the variation of the EBSD metrics KAM_a, $AMIS_a$, LAMF and DGF with applied strain in the materials plastically deformed either in tension or compression.

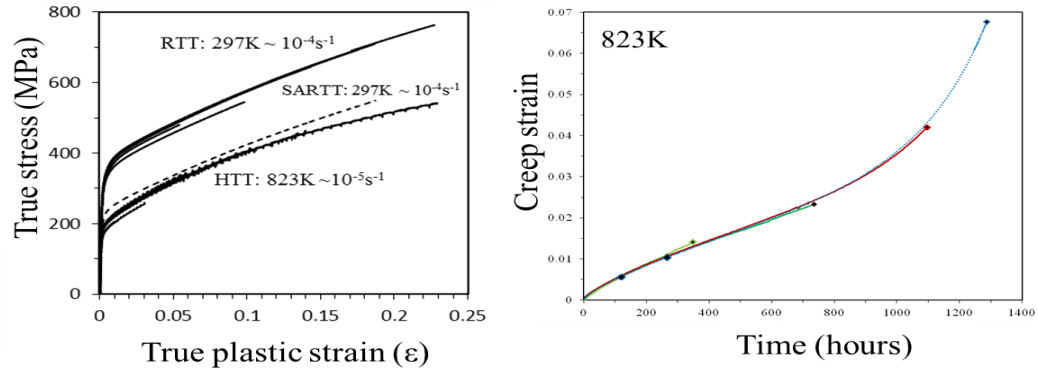

Fig.2 (a) Flow curves for ex-service and solution-annealed 316H steel, (b) Creep curves for ex-service 316H steel

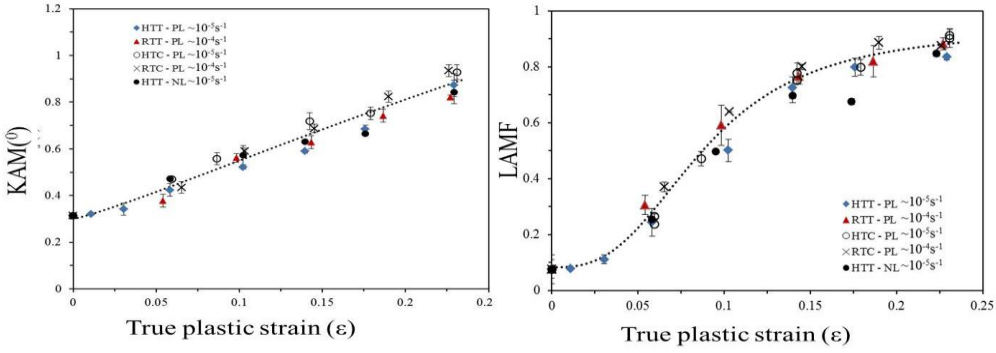

Fig .3 Variation of EBSD metrics (a) KAM_a and (b) LAMF with total plastic strain
(NL and PL refer to measurements made normal and parallel to the tensile axis)

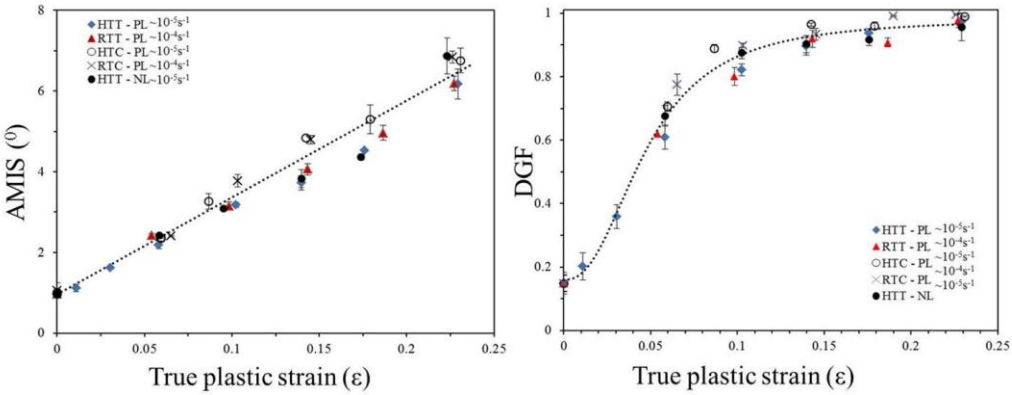

Fig.4 Variation of EBSD metrics (a) $AMIS_a$ and (b) DGF with plastic strain

The variations of the metrics KAM_a, $AMIS_a$, LAMF and DGF with increasing strain in the material deformed in creep after 8% plastic pre-strain are shown in Figs 5 and 6.

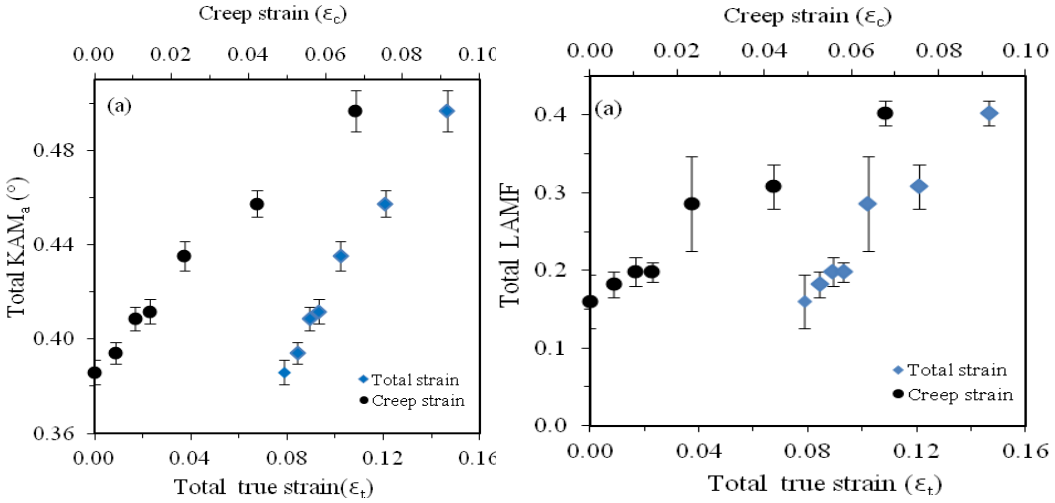

Fig 5 Variation of (a) KAM_a and (b) LAMF with strain after creep testing with pre-strain

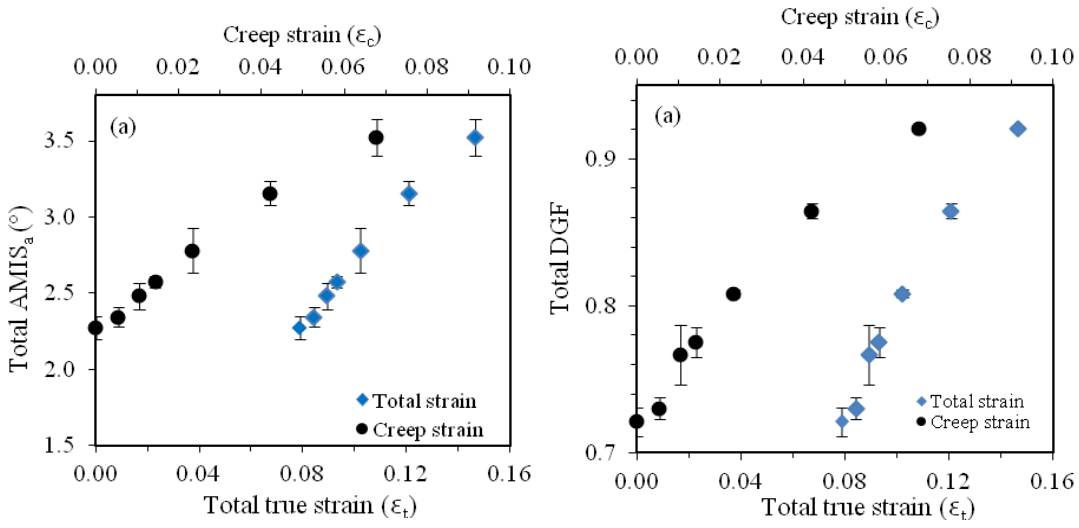

Fig 6 Variation of (a) $AMIS_a$ and (b) DGF with strain after creep testing with pre-strain

Weldment

The microstructures in the heat affected zones of the two ex-service 316H steels on either side of the weld were free of precipitates despite the base metals being aged materials. Far from the weld there was also much less precipitation than in the material of the main part of this study, but the grain boundaries were heavily attacked during the electro-polishing which may have resulted in the loss of intergranular precipitates.

The strains, at different positions close to the top, middle and bottom of each side of the weld, derived using the metric DGF (calibrated using lines fitted by regression to the DGF measurements on the mechanically tested specimens) are shown in Figs 7 and 8.

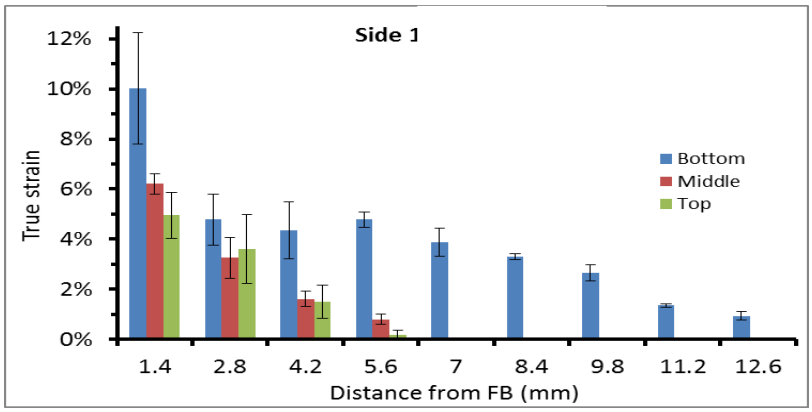

Fig.7 Estimated true plastic strain in 316H steel weldment at different distances from the fusion boundary (FB) at the positions shown in Fig.1

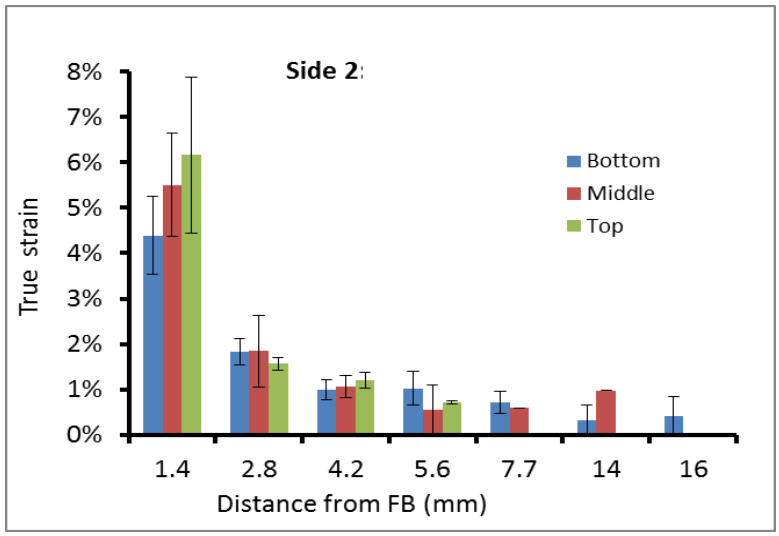

Fig.8 Estimated true plastic strain in 316H steel weldment at different distances from the fusion boundary (FB) at the positions shown in Fig.1

A comparison of the total strains in the fractured cross weld creep specimen determined using DGF and DIC measurements during the test[7] is shown in Fig.9.

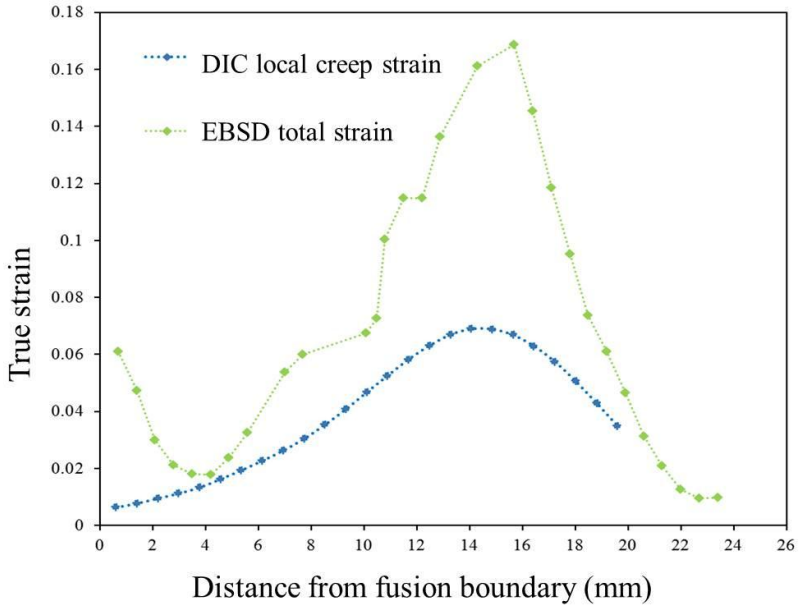

Fig. 9 Distribution of total strain in fractured cross weld creep specimen determined using DGF compared with strain measured during the test by DIC

DISCUSSION

Plastic strain

As seen in Fig2a, the flow behavior at 823K differs from that at 297K not only in that the curve shows serrations attributable to the effects of dynamic strain ageing [8, 9] but also that the flow stress is much lower at the higher temperature and the rates of strain hardening are different. Despite this, Fig.3a shows that for strain rates down to 10^{-5} s^{-1} the relationship between metric KAM_a, which is related to intragranular misorientations over distances of the order of 1μm, and known plastic strain is independent of the temperature and deformation mode. This similarity despite the difference in flow stress suggests that locally the densities of geometrically necessary dislocations are similar even though the overall dislocation densities may be different. As seen in Fig.3a the strain sensitivity of KAM_a reduces slightly for plastic strains > 0.2, this has been shown [6] to result from the nature of the metric rather than from any change in dislocation behavior.

The value of LAMF depends on the relative frequencies of low and high angle misorientations. Fig.3b shows that as the global plastic strain increases LAMF increases at a decreasing rate. This is because as deformation progresses the proportion of local misorientations classified as 'high angle' increases, reducing LAMF. At low strains LAMF is affected by orientation noise so it is most sensitive for strains $0.05 < \varepsilon < 0.15$. Like KAM_a, LAMF is insensitive to both deformation mode and the orientation of the measurement plane.

While KAM is a measure of the very local misorientations, AMIS depends on the misorientations on the scale of the whole grain and, in contrast to the bounded metrics KAM and LAMF which consider misorientations only in defined ranges, the whole range of misorientations is included when calculating $AMIS_a$. As seen in Fig.4a, $AMIS_a$ increases monotonically with strain and has good sensitivity at all strain levels.

As seen in Fig.4b the variation of DGF with strain appears unaffected by deformation temperature, mode, precipitation or the orientation of the measurement plane so may be generally applicable for 316 steels regardless of their thermal histories or grain sizes. The line fitted by regression may therefore be used as a calibration curve to determine the plastic strains in and around the heat affected zones of welds in 316 steels.

Combined plastic and creep strains

The overlay of the creep curves in Fig.2b from the 6 different ex-service 316H specimens tested shows the consistency of the creep response of this long-aged material in well-controlled tests. The effects of creep and plastic strain on the EBSD metrics are additive and comparison of Figs 3a and 5a shows that at equivalent strains developed either by plastic or creep deformation the values of the metric KAM_a were comparable. However comparisons of Figs 3, 4, 5 and 6 show that at the same strains the values of the other metrics after plastic or creep deformation were very different with LAMF, DGF and $AMIS_a$ increasing more slowly with strain developed in creep than with increasing plastic deformation. This difference between the behaviors of the different EBSD metrics, despite their all being calculated from the same orientation data, forms the basis of a new method of determining the separate contributions of prior plastic strain and the accumulated creep strain to the measured total strain in a component of unknown mechanical history [10]

Weldment

The results shown on Figs 7 and 8 indicate a general reduction of plastic strain with increasing distance from the fusion boundary (FB) from ~8% close to the inclined FB (Side 1) and ~5.5% close to the straight FB (Side 21) to close to 0% in the far field. The strain affected zone (SAZ) general extends to about 6mm from the straight FB and about 10mm from the inclined FB, extending further near the weld root. Possibly, as welding progressed, the inclination of the FB allowed the strain hardening effects of the welding thermal cycles to spread further into the base materials near the weld root than in the case of the straight FB. On the straight FB side there was no very significant strain variation in the through-thickness direction, but adjacent to the inclined FB, the geometry seemed to have a larger influence on the strain distribution, particularly near the root, where the weld experiences more thermal cycling and thus maximum deformation.

Fig.9 shows that there is good agreement between the spatial distribution of total strain in the fractured cross weld creep specimen determined using DGF and the DIC measurements of creep strain during the test. The DIC measurements of creep strain were made during the test so the strains measured by EBSD after fracture would be expected to be higher, as is seen to be the case.

CONCLUSIONS

- The EBSD metrics KAM, LAMF, AMIS and DGF can be used to determine the spatial distribution of total strain in ex-high-temperature-service (aged) 316 steel components.
- Unlike the other metrics, DGF is relatively insensitive to microstructure and can be used to determine strain where the microstructure is inhomogeneous eg around welds.
- KAM is best used for strains less than 0.2, LAMF for $0.05 < \varepsilon < 0.15$, DGF for strains up to 0.15 and AMIS is good at all strain levels examined here (up to 0.35)
- The effects of plastic and creep strain on the EBSD metrics are additive.
- KAM increases at the same rate with increasing creep strain as with plastic strain
- The other metrics respond differently to plastic and creep strain.

ACKNOWLEDGEMENTS

This project was partially funded and the materials were provided by EDF Energy

REFERENCES

[1] Lehockey, E. M. *et al*, "Mapping residual plastic strain in materials using electron backscatter diffraction" in Electron backscatter diffraction in materials science.Ed. Schwartz A. J. *et al*, Plenum (New York, 2000), pp. 247*et seq.*

[2] Angeliu, T. M. *et al* "Intergranular stress corrosion cracking of unsensitized stainless steels in BWR environments". *Proc 9th Intl Symp on Environmental Degradation of Materials in Nuclear Power Systems - Water Reactors* , New Portbeach, CA (1999).

[3] Kamaya, M. *et al* "Measurement of plastic strain of polycrystalline material by electron backscatter diffraction," Nuclear Engineering and Design Vol. 23, No. 6 (2005), pp. 713-725.

[4] Kamaya, M. *et al* "Quantification of plastic strain of stainless steel and nickel alloy by electron backscatter diffraction," Acta Mat Vol. 54 No. 2 (2006), pp. 539-548.
[5] Schwartz, A. J. *et al*, Eds. Electron Backscatter Diffraction in Materials Science, Springer, (2009).
[6] Githinji, D. N. *et al* "An EBSD Study of The Deformation of Service-Aged 316 Austenitic Steel," Met and Mat Trans A, Vol. 44, No.9 (2013), pp. 4150-4167.
[7] Sakanashi, Y. *et al* "Spatially resolved creep deformation of a thick section stainless steel welded joint" ECCC 2014 This proceedings
[8] Venugopal, S. *et al* "Optimization of cold and warm workability in stainless steel type AISI 316L using instability maps", J .Nucl. Mater. Vol. 227 Issues 1-2 (1995) pp.1-10
[9] Samuel, K.G. *et al* "Serrated yielding in AISI 316 stainless steel", Acta Metall. Vol.36 Issue8 (1988) pp. 2323-27
[10] Githinji, D. N. *et al* "An electron backscatter diffraction method for distinguishing the contributions of creep and plasticity to total strain" In preparation